Mechanisms for hydrogen diffusion in TiO_2

J. B. Bates, J. C. Wang, and R. A. Perkins*
Solid State Division, Oak Ridge National Laboratory, Oak Ridge, Tennessee 37830
(Received 22 September 1978)

The predominant hydrogen-containing species in TiO_2 (rutile) are OH^-(hydroxyl) ions, in which the oxygen occupies a regular oxygen ion site, and the O-H bond is perpendicular to the c axis. It is proposed that diffusion of hydrogen parallel to the c axis proceeds by a proton jump from one O^{2-} ion to another along the channel as represented by $OH^-\cdots O^{2-} \rightarrow O^{2-}\cdots H^+\cdots O^{2-} \rightarrow O^{2-}\cdots HO^-$. It is also proposed that diffusion perpendicular to the c axis proceeds by a rotation of the OH^- bond to move the proton from one channel to an adjacent channel, followed by a proton jump to another O^{2-} ion in the same channel. From a potential-energy model, which includes a Morse function to represent the OH^- bond, as well as electrostatic and repulsive terms, the activation energies for hydrogen and tritium diffusion parallel to the c axis were calculated to be (including a zero-point energy correction) 0.60 and 0.69 eV, respectively, in good agreement with the respective experimental values of 0.59 and 0.75 eV. The calculated activation energy for diffusion perpendicular to the c axis was 1.23 eV (no zero-point energy correction), as compared to the experimental values of 1.28 and 1.11 eV, respectively, for hydrogen and tritium. The calculated equilibrium orientation of the OH^- ion in TiO_2 and the calculated stretching frequency of this species were also in good agreement with the respective experimental results.

I. INTRODUCTION

The results from infrared measurements on TiO_2 (rutile) containing hydrogen, deuterium, and tritium and the results from diffusivity measurements of tritium in rutile have been described in two earlier publications from this laboratory.[1,2] Based on these studies, we proposed a mechanism[3] for the diffusion of hydrogen and its isotopes parallel and perpendicular to the c axis in TiO_2. A model has been developed for OH^- in TiO_2 which provides calculated activation energies for diffusion parallel and perpendicular to the c axis in good agreement with the experimental values.[2,4] Furthermore, the model accurately predicts the equilibrium orientation of hydrogen in rutile, and the calculated OH^- stretching frequency agrees well with the observed value. The purpose of this paper is to discuss this model and the mechanisms for hydrogen diffusion in TiO_2.

The diffusion of hydrogen and its isotopes in rutile has been investigated by several groups.[2-7] A comparison of the results from these studies was made recently[2] and will not be repeated here. The possible reactions which occur when hydrogen enters TiO_2 from a vapor phase of H_2O or H_2 and the thermodynamics of hydrogen solubility in rutile have been discussed in detail.[8,9] In our study, we have not considered the mechanism of how hydrogen enters rutile, but rather we modeled the processes by which hydrogen is transported through the lattice.

II. REVIEW OF EXPERIMENTAL RESULTS

A. Spectroscopic studies

A perspective drawing of the rutile lattice is shown in Fig. 1. The small open circles represent Ti^{4+} ions and the large open circles represent O^{2-} ions. Rutile has a tetragonal structure which belongs to the space group D_{4h}^{14}. The lattice constants[10] at 25 °C are $a_0 = 4.594$ Å and $c_0 = 2.958$ Å. The structure is characterized by large open channels parallel to the c axis as shown in Fig. 1. These channels account for the fact that light interstitial ions diffuse much more rapidly parallel to the c axis than perpendicular to the c axis.[2,4,11]

Measurements of the infrared-absorption spectra of hydrogen and its isotopes in TiO_2 have shown[1,8,12,13] that most of the hydrogen which enters the lattice on heating rutile crystals in an environment of H_2 or H_2O is bound in the form of OH^- ions.[14] It was suggested by von Hippel *et al.*[8] that the proton binds to an O^{2-} ion of the rutile lattice. The large dichroism found for the OH^- absorption[12] (>99% absorption perpendicular to c) indicates that the transition moment, and therefore the OH bond, is perpendicular to the c axis. This result was verified in an EPR study[15] of Fe^{3+} in TiO_2. From an analysis of the spectra, the proton was determined to be located at (0.53, 0.11, 0.0) in fractional coordinates, where the O^{2-} to which it is bonded is located at (0.8053, 0.3053, 0.0). The O–H bond length was determined to be 1.09 Å. The calculated position of the proton is very near

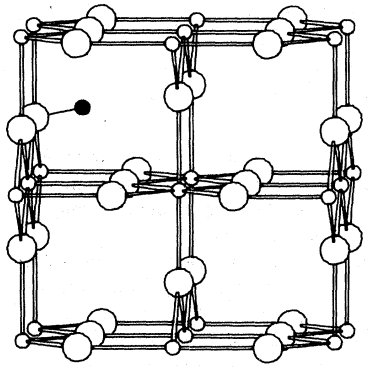

FIG. 1. Rutile lattice showing calculated position of the proton (solid circle). The large open circles represent O^{2-} ions and the small open circles represent Ti^{4+} ions.

to the experimental position (see below) and is shown in Fig. 1, where the small closed circle represents H^+, and the bond is drawn to the O^{2-} ion located ~1 Å away. The proton may be bound to any O^{2-} ion, so that a projection of the OH bonds onto the (001) plane will show that they are related by 90° rotations about an axis parallel to c_0 and located in the center of the channel. This orientation of OH^- dipoles around the channel is consistent with the observation of isotropic absorption from the OH^- when infrared light is incident along the [001] direction.[1]

The origin of the large frequency shift of the OH^- stretching mode in TiO_2, $\nu_H = 3276$ cm^{-1} at 300 K, compared to a nominal free-ion value of ~3600 cm^{-1} was not explained in the previous spectroscopic studies.[1,8,12,13] It was noted[8] that, if the shift is due to hydrogen bonding represented by OH···O, the oxygen-oxygen separation is required to be about 2.75 Å. Therefore, von Hippel *et al.*[8] were prompted to place the proton along the line joining the O^{2-} ions that are separated by 2.779 Å. This orientation places the O–H bond out of the (001) plane, in contradiction to the experimental and calculated results. Furthermore, the comparatively narrow bandwidths observed[1] for OH^-, OD^-, and OT^- in TiO_2 are not consistent with a linear hydrogen bond having an O···O separation of 2.75 Å or less.[16,17] The proton position in Fig. 1 corresponds to a nearly linear hydrogen bond with an O···O separation of 3.327 Å, and virtually no shift from the free-ion frequency is predicted from such a weak H bond.[17]

TABLE I. Spectroscopic constants for OH^-, OD^-, and OT^- in TiO_2.[a]

	ω_e (cm^{-1})	$\omega_e x_e$ (cm^{-1})	$G_e(0)$ (eV)
OH^-	3545.14	134.57	0.22
OD^-	2579.44	71.24	0.16
OT^-	2163.95	50.14	0.13

[a] Constants for $T = 300$ °K from Ref. 1.

The measured stretching frequencies of OH^-, OD^-, and OT^- were analyzed in a previous study[1] using a term-value formula for a diatomic anharmonic oscillator,[18]

$$G_e^i(v) = (v+\tfrac{1}{2})\omega_e^i - (v+\tfrac{1}{2})^2\omega_e^i x_e^i, \quad (1)$$

where $G_e^i(v)$ is the observed vibrational energy for the ith isotope, v is the vibrational quantum number, and ω_e^i and x_e^i are constants for the ith isotope. The values of the spectroscopic constants derived from Eq. (1) which are used in the present study are summarized in Table I. The zero-point energy for the ith isotope is [from Eq. (1)]

$$G_e^i(0) = \tfrac{1}{2}\omega_e^i - \tfrac{1}{4}\omega_e^i x_e^i. \quad (2)$$

B. Diffusion measurements

The Arrhenius equations for diffusion parallel to the c axis as determined from the measured diffusivities are

$$D_{\parallel}(H) = 1.8(\pm 0.8) \times 10^{-3} \exp[-0.59(\pm 0.02)/kT] \text{ cm}^2/\text{sec} \quad (3)$$

for hydrogen,[4] and

$$D_{\parallel}(T) = 8.5(\pm 9.0) \times 10^{-3} \exp[-0.75(\pm 0.06)/kT] \text{ cm}^2/\text{sec} \quad (4)$$

for tritium,[2] with the activation energy expressed in eV. The uncertainties quoted for the preexponential factors and activation energies correspond to 90% confidence levels. The justification for comparing the hydrogen and tritium diffision coefficients, which were measured by different techniques, was discussed in detail previously.[2] It depends on the minimization of the effects of internal electric fields in both experiments.[4] The difference between the zero-point energies of the OH^- and OT^- stretching vibrations determined at 300 K (Table I), $0.22 - 0.13 = 0.09$ eV, is of the order of the difference between the activation energies for tritium and hydrogen diffusion parallel to the c axis, $0.75 - 0.59 = 0.16 \pm 0.08$ eV considering the uncertainty of the latter quantity. This suggests that the activation energy for diffusion along the c axis is mainly determined by the energy required to break the OH^- bond in TiO_2. The diffusion process in this case consists of proton jumps from one O^{2-} ion to another, as represented by

$$OH^- \cdots O^{2-} \rightarrow O^{2-} \cdots H^+ \cdots O^{2-} \rightarrow O^{2-} \cdots HO^-. \quad (5)$$

The Arrhenius equations reported for diffusion

perpendicular to the c axis are given by

$$D_{\perp}(\mathrm{H}) = 3.8(\pm 2.0) \times 10^{-1} \exp[-1.28(\pm 0.05)/kT] \ \mathrm{cm}^2/\mathrm{sec} \quad (6)$$

for hydrogen,[4] and by

$$D_{\perp}(\mathrm{T}) = 1.77(\pm 1.0) \times 10^{-2} \exp[-1.11(\pm 0.04)/kT] \ \mathrm{cm}^2/\mathrm{sec} \quad (7)$$

for tritium.[2] The activation energies for diffusion of hydrogen and tritium perpendicular to c are much larger than the respective values for diffusion parallel to c. This implies that a different mechanism is responsible for the rate-determining step in diffusion perpendicular to c, and it was proposed[3] that this step consists of a flip over or rotation which moves the proton from one channel to another.

III. MODEL FOR OH^- IN TiO_2

Our major goal in this research was to develop a model for OH^- in TiO_2 from which we could calculate the activation energies and preexponential factors for diffusion based on the mechanisms outlined above. The model was also required to provide results consistent with other known physical properties such as the orientation, bond length, and stretching frequency of OH^- in TiO_2. It was assumed that the oxygen atom of the hydroxyl ion occupies an O^{2-}-ion site of the rutile lattice. The charge distribution in the OH^- ion was estimated from the electron-density contours calculated by Bader[19] using Cade's[20] electronic wave functions for OH^-. The radius of H^+ was estimated to be 0.83 Å when the radius of O^{2-} was taken to be 1.40 Å. From Bader's contours, the electrons have approximately spherical distributions centered about the oxygen and hydrogen nuclei. The number of electrons contained in that half of the sphere about O^{2-} away from the proton was found to be 4.68. Thus, based on the assumption of two spherical charge distributions, there are 9.36 electrons in the sphere about O^{2-} and 0.64 electrons in the sphere about H^+, since OH^- has a total of ten electrons. With $Z=8$ for O^{2-} and $Z=1$ for H^+, this gives a net charge of -1.36 centered on the oxygen nucleus and $+0.36$ centered on the H^+ nucleus.

Because of the strong bond between the proton and the oxygen ion in OH^-, we found that it was necessary to represent the O–H interaction by means of a Morse potential[21] or other similar functions which are ordinarily used as potentials for diatomic molecules.[22] The function we found to give acceptable results is given by

$$V = \sum_i D_e\{1 - \exp[-a(r_{ih} - r_e)]\}^2 - \sum_{i\neq 0} \frac{q_h \vec{r}_{ih} \cdot \vec{p}_i}{r_{ih}^3} + \sum_j \frac{q_h q_j}{r_{jh}} + \sum_j b\epsilon \exp\left(-\frac{1}{\rho}(r_{jh} - R_h - R_j)\right). \quad (8)$$

The index i labels O^{2-} ions only, where $i=0$ denotes the O^{2-} ion in OH^-, and the index j labels only Ti^{4+} ions. The distance between the proton and the kth ion ($k=i$ for O^{2-} and $k=j$ for Ti^{4+}) is denoted by r_{kh}, with $r_{kh} = |\vec{r}_{kh}| = |\vec{r}_k - \vec{r}_h|$, where $\vec{r}_k$ and $\vec{r}_h$ are the position vectors of the kth ion and proton, respectively.

The first term in Eq. (8) is the Morse function,[21] which represents the major part of the O–H potential. The constant D_e is the energy measured from the minimum of this function to its horizontal asymptote (the dissociation limit in the case of the free ion), r_e is the equilibrium O–H bond length, and a is a parameter which, together with D_e, determines the curvature of the potential near $r_{ih} = r_e$. The value of $D_e = 3.484$ eV was taken from Cade's calculation of energy as a function of internuclear distance (Table III of Ref. 20). The value of $a = 2.891$ Å^{-1} was determined from the relationship,[22] $a = (k_e/2D_e)^{1/2}$, where $k_e = 9.334 \times 10^5$ dyn/cm is the calculated force constant[20] of OH^-. The value of $r_e = 0.97$ Å quoted by Branscomb[23] gave better results than the calculated value[20] of 0.94 Å.

The second term in Eq. (8) arises from the interaction of the charge on the proton q_h, with the induced dipole moments on the O^{2-} ions, $\vec{p}_i$. The induced moment was determined from the following procedure.[24] A unit dipole p_0 was placed along the x axis of a test O^{2-} ion giving a dipole moment of $\vec{p}_1 = p_0\hat{i}$ on this ion, where $\hat{i}$ is a unit vector along x. Crystal symmetry was used to find the corresponding dipole moments on all other O^{2-} ions. The electric field at the test ion produced by these other dipole moments is given by $\vec{E}_1 = (E_{1x}, E_{1y}, E_{1z})$. This procedure was repeated with unit dipole moments along the y and z axes of the test ion, $\vec{p}_2 = p_0\hat{j}$ and $\vec{p}_3 = p_0\hat{k}$, and the corresponding electric fields calculated at the test ion are given by $\vec{E}_2 = (E_{2x}, E_{2y}, E_{2z})$ and $\vec{E}_3 = (E_{3x}, E_{3y}, E_{3z})$. The net dipole moment at the O^{2-} ion can be written

$$\vec{p} = p_x\hat{i} + p_y\hat{j} + p_z\hat{k}. \quad (9)$$

This moment is induced by the electric field due to point charges of all the other ions $\vec{E}_0$ and by the electric field due to induced dipole moments on all the other O^{2-} ions. Thus,

$$\vec{p} = \alpha_0[\vec{E}_0 + (1/p_0)(p_x\vec{E}_1 + p_y\vec{E}_2 + p_z\vec{E}_3)], \quad (10)$$

where $\alpha_0 = 2.22$ Å^3 is the polarizability of O^{2-} in TiO_2.[25] In Eq. (10), p_x/p_0, p_y/p_0, and p_z/p_0 are

scaling factors which determine the magnitude of the respective electric fields due to induced dipole moments along x, y, and z, respectively. A set of three simultaneous equations is given by Eqs. (9) and (10):

$$\begin{aligned} p_x &= \alpha_0[E_{0x}+(1/p_0)(p_xE_{1x}+p_yE_{2x}+p_zE_{3x})]\,, \\ p_y &= \alpha_0[E_{0y}+(1/p_0)(p_xE_{1y}+p_yE_{2y}+p_zE_{3y})]\,, \\ p_z &= \alpha_0[E_{0z}+(1/p_0)(p_xE_{1z}+p_yE_{2z}+p_zE_{3z})]\,. \end{aligned} \tag{11}$$

These equations were solved for p_x, p_y, and p_z. From a lattice-sum calculation, $|\vec{E}_0| = 0.1968\ e/\text{Å}^2$, $|(1/p_0)(p_x\vec{E}_1+p_y\vec{E}_2+p_z\vec{E}_3)| = 0.1661\ e/\text{Å}^2$, and the net dipole moment at the O^{2-} ion was found to have the magnitude, $|\vec{p}| = 0.692\ e\,\text{Å}$(3.32 D).

The third term in Eq. (8) arises from the Coulomb interaction between the charge on the proton $q_h = +0.36$ and the charge on the titanium ions $q_j = +4$. The Coulomb interaction between the charge on the O^{2-} ions and the Ti^{4+} ions was not included, since this contributes only a constant energy term under the assumption that the O^{2-} and Ti^{4+} ions remain fixed.

The last term in Eq. (8) accounts for the short-range repulsive interaction between the OH^- and the titanium ions.[26] The terms due to oxygen-oxygen, oxygen-titanium, and titanium-titanium contacts were omitted, since these contribute a constant energy when only the proton is allowed to move. The constants R_h and R_j are, respectively, the ionic radius of the proton and Ti^{4+}. The latter was taken to have the value $R_j = 0.68$ Å while, from the model of OH^- described above, $R_h = 0.83$ Å. The values of ρ found by Tosi and Fumi[26] for alkali halides are in the range of 0.282–0.386 Å. Here its value was taken to be 0.333 Å. The parameter ϵ is defined by $\epsilon = \epsilon_{jh} = 1 + Z_j/N_j + Z_h/N_h$, where Z and N are the valence and number of electrons in the last closed shell, respectively. For Ti^{4+}, $Z_j = 4$ and $N_j = 8$, and for the OH^- ion, $Z_h = -1$ and $N_h = 8$, these give $\epsilon = 1.375$. Using the value of $\rho = 0.333$ Å, the parameter b was determined from a calculation of the perfect-crystal potential energy of an O^{2-} ion near its equilibrium position $\vec{r}_0$,

$$V = -\sum_{i\neq 0}\frac{q_0\vec{r}_{0i}\cdot\vec{p}_i}{r_{0i}^3}+\sum_{k\neq 0}\frac{q_0q_k}{r_{0k}} + \sum_{k\neq 0} b\epsilon_{0k}\exp[-(1/\rho)(r_{0k}-R_0-R_k)]\,, \tag{12}$$

where the sum over k includes all the ions and $i = 0$ and $k = 0$ denote the O^{2-} ion at $\vec{r}_0$. The value of b was found by requiring the O^{2-} ion to be located at its equilibrium position in the crystal. This calculation gave $b = 0.58$ eV.

TABLE II. Parameter values for the potential energy model of OH^- in TiO_2.

$D_e = 3.484$ eV	$q_h = +0.36$	$b = 0.58$ eV
$a = 2.891\ \text{Å}^{-1}$	$\lvert\vec{p}\rvert = 0.692\ e\,\text{Å}$	$\epsilon = 1.375$
$r_e = 0.97$ Å	$R_{Ti^{4+}} = 0.68$ Å	$R_h = 0.83$ Å
	$\rho = 0.333$ Å	

The values of the parameters in Eq. (8) are collected in Table II. As noted above these were determined from known properties of TiO_2 and from calculations of the electronic structure of a free OH^- ion. They were used without further adjustment to give the calculated results described below.

IV. RESULTS OF THE CALCULATIONS

A. Orientation and vibrational frequencies

The equilibrium orientation of the proton was calculated by finding the minimum-energy position as the proton was moved under the potential field given in Eq. (8). This position was determined to be[27] (0.57, 0.12, 0.0) in fractional coordinates. The equilibrium O-H-bond length was calculated as $r_e = 1.03$ Å. The calculated position and bond length agree well with the experimental values, (0.56, 0.11, 0.0) and $r_e = 1.09$ Å, determined from the EPR spectra[15] of Fe^{3+} in TiO_2. The lengthening of the OH bond in the TiO_2 lattice compared to the isolated ion ($r_e = 0.97$ Å) is caused by the electrostatic fields in the crystal as represented by the second and third terms in Eq. (8).

The O-H stretching frequency was estimated by calculating numerically the second derivative of V with respect to r near $r = r_e$ and using the harmonic-oscillator relation, $d^2V/dr^2 = k_e = 4\pi^2c^2\mu\omega_e^2$. The derivative was calculated in increments of $\Delta r = 0.01$ Å, and the result gave $\omega_e = 3182\ \text{cm}^{-1}$. The calculated frequency agrees within 10% of the experimental value determined from the 300 K data $\omega_e = 3545\ \text{cm}^{-1}$ (Table I). The model represented by Eq. (8) accounts for the large negative shift of the stretching frequency of OH^- in TiO_2 from the free-ion value and resolves the previous conflicts in interpreting the spectroscopic data (frequency shift and bandwidth) on the basis of hydrogen bonding. The model shows that the electrostatic interactions of OH^- in TiO_2 (second and third terms in Eq. (8)) are responsible for the relaxation of the O-H bond resulting in a decrease in the stretching frequency as well as an increase in the bond length. Hydrogen bonding, therefore, does not play an important role in this case.

Frequencies for librational displacements of the

TABLE III. Calculated and observed equilibrium properties of OH^- in TiO_2.

	Observed	Calculated
Orientation[a]	(0.56,0.11,0.0)	(0.57,0.12,0.0)
Bond length (Å)	1.09[d]	1.03
OH stretching[b] (cm^{-1})	3545[e]	3182
Libration,[c] $\perp$ (cm^{-1})		1427
Libration,$\parallel$ (cm^{-1})		719

[a] Fractional coordinates.
[b] Harmonic values, ω_e.
[c] Librational frequencies for displacements perpendicular ($\omega_\perp$) and parallel ($\omega_\parallel$) to the c axis.
[d] Reference 15.
[e] Reference 1 and Table I.

OH^- ion parallel and perpendicular to the c axis, $\omega_\parallel$ and $\omega_\perp$, respectively, were calculated using a procedure analogous to that described above. It is assumed that the OH-bond length remains fixed and that displacements occur about axes passing through the center of the oxygen atom. The calculations gave $\omega_\parallel = 1427\ cm^{-1}$ and $\omega_\perp = 719\ cm^{-1}$. There are no experimental values for the librational frequencies of OH^- in TiO_2, but the librational mode of OH^- in $Ca(OH)_2$ has been observed[28] at 680 cm^{-1}. The calculated equilibrium properties of OH^- are collected in Table III together with the available measured values.

B. Diffusion paths and activation energies

1. Diffusion parallel to c axis

Our mechanism for hydrogen diffusion parallel to the c axis involves a jump of the proton from one O^{2-} ion to another along the channel, as represented by Eq. (5). In order to determine the minimum-energy path and the barrier height of this path, the proton was moved in increments of 0.17 Å subject to the potential of Eq. (8) along a line from a calculated initial equilibrium position to each of the calculated equilibrium positions associated with neighboring O^{2-} ions. After each displacement, the minimum-energy position of the proton in the plane perpendicular to the direction of displacement was determined. The process of displacement followed by location of the minimum-energy position was carried out until the proton reached the midpoint of the path between the initial and final equilibrium locations. The locus of points generated by this procedure defines the diffusion path, and the difference between the energies at the midpoint and the initial position is the barrier height. The diffusion path determined from our calculations is illustrated in Fig. 2; the barrier height for this path is $E_b = 0.824$ eV. All other paths gave significantly larger barrier heights. For example, the calculated barrier height for a proton jump to the O^{2-} ion directly across the channel from the origin ion is 1.13 eV.

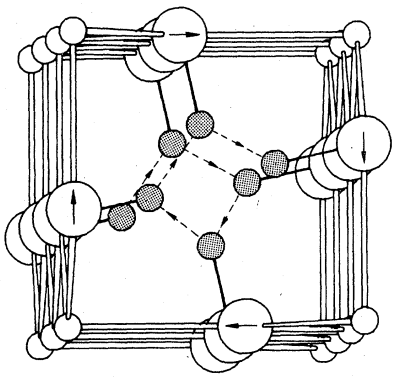

FIG. 2. Calculated path for diffusion of hydrogen parallel to the c axis. The equilibrium hydrogen positions are indicated by shaded circles with a bond to the appropriate O^{2-} ion. The direction of proton diffusion is indicated by the arrows along the path. The orientations of the dipole moments on the O^{2-} ions are indicated by the arrows within the large open circles.

The diffusion path in Fig. 2 describes a helix as the proton moves along the channel. The geometry of this path is mainly determined by the orientation of the induced dipole moments on the O^{2-} ions. The orientations of these moments are illustrated by the arrows on the O^{2-} ions in Fig. 2. The H^+ ion moves in a direction away from the positive end of the dipole (point of the arrow) on the origin ion toward the negative end of the dipole on the neighboring O^{2-} in the adjacent (001) plane.

The activation energy for diffusion is given by the difference in the barrier height and the zero-point energy:

$$E_a = E_b - E_0 . \tag{13}$$

(A discussion of the importance of the zero-point energy to the isotope effect in diffusion parallel to c is given in the Appendix.) As noted above, the difference in zero-point energies between the OH^- and OT^- stretching modes (0.09 eV at 300 K) is of the order of the difference between the activation energies for tritium and hydrogen diffusion parallel to c (0.16 ± 0.08 eV), considering the uncertainties in the latter quantities. That this should be true follows from the diffusion mechanism. The activation energies calculated from Eq. (13) using the experimental zero-point energies of the stretching modes (Table I) are listed together with the observed values in Table IV.

A more exact calculation of the activation energies would include the zero-point energies of all of the modes (lattice and local proton modes) in the equilibrium state and saddle-point configura-

TABLE IV. Observed and calculated activation energies for diffusion of hydrogen, deuterium, and tritium parallel and perpendicular to the c axis in TiO_2.

(a) Diffusion parallel to c

	Activation energy (eV) Observed	Calculated [a] (1)	(2)
H	0.59(±0.02) [b]	0.60	0.64
D	0.59 [b]	0.66	0.69
T	0.75(±0.06) [c]	0.69	0.71

(b) Diffusion perpendicular to c

	Activation energy (eV) Observed	Calculated [d]
H	1.28(±0.05) [b]	
D	1.28 [b]	1.23
T	1.11(±0.04) [c]	

[a] Values under (1) calculated from Eq. (13) using experimental zero-point energies for stretching mode. Values under (2) calculated from Eq. (14) using calculated frequencies at the equilibrium and saddle-point positions.
[b] Reported in Ref. 4.
[c] Reported in Ref. 2.
[d] Activation energies equal to barrier height within 0.001 eV.

TABLE V. Calculated zero-point energies for the equilibrium and saddle-point positions for hydrogen in TiO_2.

(a) Diffusion parallel to c

Mode k	Energy (eV) [a] $G_{e,k}(0)$	$G'_{e,k}(0)$	$G_{e,k}(0) - G'_{e,k}(0)$
1	0.197	0	0.197
2	0.088	0.099	−0.011
3	0.045	0.052	−0.007
			$\sum_k = 0.179$

(b) Diffusion perpendicular to c

Mode k	Energy (eV) [b] $G_{e,k}(0)$	$G'_{e,k}(0)$	$G_{e,k}(0) - G'_{e,k}(0)$
1	0.197	0.188	0.009
2	0.088	0.141	−0.053
3	0.045	0.0	0.045
			$\sum_k = 0.001$

[a] Calculated saddle-point frequencies are $\omega'^{(2)}_e = 1590$ cm^{-1} and $\omega'^{(3)}_e = 832$ cm^{-1}.
[b] Calculated saddle-point frequencies are $\omega'^{(1)}_e = 3032$ cm^{-1} and $\omega'^{(2)}_e = 2281$ cm^{-1}.

tion:

$$E_a = E_b - \sum_{k=1}^{N} G_{e,k}(0) + \sum_{k=1}^{N-1} G'_{e,k}(0)\,, \qquad (14)$$

where $G_{e,k}(0)$ and $G'_{e,k}(0)$ are the zero-point energies of the kth mode in the equilibrium and saddle-point states, respectively, and N is the number of normal modes (see Appendix). In the present approximation we include only the motion of the proton so that $N = 3$. The vibrational frequencies of the two modes of the proton at the halfway point of the path for c-axis diffusion were calculated from the numerical second derivatives of the potential with respect to the displacements perpendicular to the path. The results are $\omega'_e(2) = 1590$ cm^{-1} and $\omega'_e(3) = 832$ cm^{-1} for H^+. Using these frequencies together with those calculated for the equilibrium position, the activation energies for hydrogen, deuterium, and tritium diffusion were calculated from Eq. (14), and the results are listed in Table IV. For this calculation, the zero-point energies were taken to be $G_{e,k}(0) = \frac{1}{2}\omega_e(k)$ and $G'_{e,k} = \frac{1}{2}\omega'_e(k)$, with ω_e and ω'_e expressed in eV, and the frequencies of the D^+ and T^+ isotopes were determined by scaling the H^+ frequencies with the appropriate reduced mass factor, $(\mu_H/\mu_D)^{1/2}$ and $(\mu_H/\mu_T)^{1/2}$, respectively. In Table V a, we compare the calculated zero-point energies of each mode in the equilibrium and saddle-point states for hydrogen. As expected, these data show that the dominant contribution to the difference between the equilibrium and saddle-point zero-point energies comes from the stretching mode.

2. *Diffusion perpendicular to c axis*

The mechanism we propose for diffusion of hydrogen perpendicular to the c axis consists of a flip over or rotation of the OH^- ion which moves the proton from one channel to an adjacent channel. The combination of a flip over and a jump diffusion along the channel results in a net transport of H^+ perpendicular to the c axis. The diffusion path was calculated by rotating the basal plane containing the proton by 10° increments about an axis connecting the O^{2-} ion and a neighboring Ti^{4+} ion in the same basal plane. After each incremental rotation, the minimum-energy position of the proton in the plane was calculated. As a result of these adjustments to minimize the energy, the OH-bond length increased from 1.026 Å at the equilibrium position ($\theta = 0°$) to 1.043 Å at $\theta = 50°$, and then decreased to 1.021 Å at the saddle point ($\theta = 90°$). The diffusion path calculated by this method is illustrated in Fig. 3. The barrier height for the diffusion path is $E_b = 1.23$ eV.

The experimental activation energies given in Eqs. (6) and (7) have $E_a(H) > E_a(T)$, and the differ-

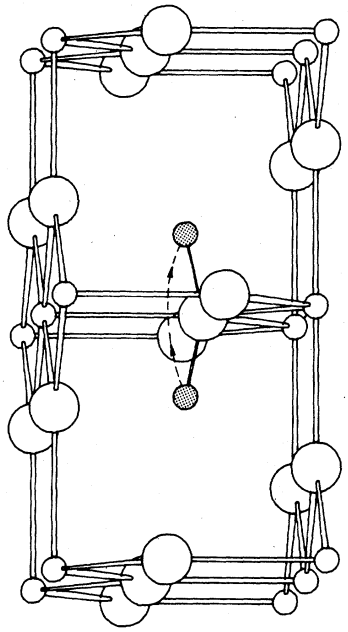

FIG. 3. Calculated path for the flip over or rotation mechanism for diffusion of hydrogen perpendicular to the c axis.

ence between them is larger than the uncertainty limits; $E_a(\mathrm{H}) - E_a(\mathrm{T}) = 0.17 \pm 0.09$ eV. Based on our model and the discussion in the Appendix, we would predict an opposite ordering of the activation energies: $E_a(\mathrm{T}) \geq E_a(\mathrm{H})$. In contrast to the case for diffusion parallel to c, there are no experimental librational frequencies from which to estimate a zero-point energy correction for diffusion perpendicular to c. The frequencies of the two modes at the saddle point were calculated by the method described above. These were found to be $\omega_e'(1) = 3032$ cm^{-1} and $\omega_e'(2) = 2281$ cm^{-1}, for the stretching mode and a librational mode respectively. The zero-point energies for the equilibrium and saddle-point states are listed in Table V b. The zero-point energy correction to E_b given by the sum of the terms in the last column is a negligibly small number compared to the uncertainties in the measured activation energies. Therefore, we take $E_a = 1.23$ eV as the calculated activation energy for diffusion perpendicular to c. This value is compared with the experimental results in Table IV b.

C. Preexponential factors

A random-walk model for thermally activated diffusion in one direction gives

$$D_0 = \tfrac{1}{2}\nu_a d^2 \qquad (15)$$

for the preexponential factor of the Arrhenius expression, where d is the jump distance and ν_a is the number of attempts made at surmounting the barrier (attempt frequency). Johnson *et al.*[4] made estimates of the attempt frequencies for hydrogen. For diffusion parallel to c, they assumed a jump distance of 1.48 Å ($\frac{1}{2}c_0$) and estimated that $D_0 = 2.3 \times 10^{-3}$ cm^2/sec, in good agreement with the observed value[4] of 1.8×10^{-3} cm^2/sec. For diffusion perpendicular to c, they assumed a jump distance of 3.26 Å ($a_0/\sqrt{2}$) and estimated that $D_0 = 3.4 \times 10^{-2}$ cm^2/sec. The latter estimate is about an order of magnitude smaller than their reported value of 3.8×10^{-1} cm^2/sec.

The attempt mode for diffusion parallel to c must cause the proton to be displaced parallel to the c axis. The librational motion of OH^- parallel to c satisfies this requirement, and, since two attempts are made at the barrier on each cycle of this mode, $\nu_a(\|c) = 2\omega_{\|}$. Using the calculated value of $\omega_{\|}$ (2.16×10^{13} sec^{-1}) and $d = \frac{1}{2}c_0$, Eq. (15) gives $D_0 = 4.7 \times 10^{-3}$ cm^2/sec for hydrogen and $D_0 = 2.7 \times 10^{-3}$ cm^2/sec for tritium. These values are compared with the observed preexponential factors in Table VI.

The preexponential factors for hydrogen and tritium diffusion perpendicular to c, 3.8×10^{-1} and 1.77×10^{-2} cm^2/sec, respectively,[2,4] are more than an order of magnitude larger than their corresponding factors for diffusion parallel to c. The difference in jump distances accounts for about a factor-of-5 difference between the respective pre-

TABLE VI. Observed and calculated preexponential factors for diffusion of hydrogen, deuterium, and tritium parallel and perpendicular to the c axis in rutile.

(a) Diffusion parallel to c

	D_0 (cm^2/sec) Observed[a]	Calculated[c]
H	$1.8(\pm 0.8) \times 10^{-3}$	4.7×10^{-3}
D	(1.3×10^{-3})[b]	3.3×10^{-3}
T	$8.5(\pm 9.0) \times 10^{-3}$	2.7×10^{-3}

(b) Diffusion perpendicular to c

	D_0 (cm^2/sec) Observed[a]	Calculated[c]
H	$3.8(\pm 2.0) \times 10^{-1}$	4.5×10^{-2}
D	(2.7×10^{-1})[b]	3.2×10^{-2}
T	$1.77(\pm 1.0) \times 10^{-2}$	2.6×10^{-2}

[a] Observed values for hydrogen and tritium from Refs. 4 and 2, respectively.

[b] The D_0 for deuterium was assumed to be given by $D_0(D) = D_0(H)/\sqrt{2}$.

[c] The calculated values for deuterium and tritium were taken to be $D_0(\mathrm{D}) = D_0(\mathrm{H})/\sqrt{2}$ and $D_0(\mathrm{T}) = D_0(\mathrm{H})/\sqrt{3}$, respectively.

exponential terms, so that the attempt frequencies for diffusion perpendicular to c must be larger than those for diffusion parallel to c. At the present time, it is not clear what mode or combination of modes leads to attempts at diffusion perpendicular to c. We have assumed that both librational modes are involved: two attempts are made for each cycle of $\omega_{\parallel}$ and one attempt is made for each cycle of $\omega_{\perp}$. With this assumption, $\nu_a(\perp c) = 2\omega_{\parallel} + \omega_{\perp}$. Using the calculated values of $\omega_{\parallel}$ and $\omega_{\perp}$ from Table III expressed in sec^{-1} and assuming $d = a_0/\sqrt{2}$, Eq. (15) gives $D_0 = 4.5 \times 10^{-2}$ cm^2/sec for hydrogen and $D_0 = 2.6 \times 10^{-2}$ cm^2/sec for tritium. A comparison of the observed and calculated preexponential factors given in Table VI shows that a reasonably good result was obtained for D_0 of tritium, especially considering the uncertainty of the experimental value. The poor agreement with the observed D_0 for hydrogen may be due to a larger experimental uncertainty than quoted.[4] The Arrhenius equation for diffusion of H perpendicular to c was derived from only four data points measured over a narrow temperature range. If the observed tritium preexponential factor is multiplied by $\sqrt{3}$, the "experimental" factor for hydrogen becomes $D_0(H) = 3.1 \times 10^{-2}$ cm^2/sec. It is seen that our estimate of $D_0(H)$ as well as that of Johnson *et al.*[4] agrees much better with $D_0(H)$ based on the tritium data than with the experimental value reported in Ref. 4.

V. DISCUSSION AND CONCLUSIONS

The contributions to the calculated barrier-height energy for the diffusion mechanisms parallel and perpendicular to the c axis from the four terms in Eq. (8) are listed in Table VII. It is no surprise that the Morse potential contributes the dominant term to $E_b(\|c)$, since the mechanism involves breaking an O-H bond. The Coulomb term is necessarily the largest contributor to $E_b(\perp c)$ since the positively charged proton moves through a region of neighboring Ti^{4+} ions. The repulsive term is also appreciable because of the close nearest neighbor contacts along the diffusion path.

The disagreement between the measured activation energies for diffusion of hydrogen and tritium perpendicular to the c axis is likely due to experimental errors in both measurements.[2,4] The calculations suggest that the activation energies should be equal, since the zero-point energy correction is negligible in this case. The calculated activation energy agrees better with the experimental value for hydrogen than it does with that for tritium. However, we believe the tritium activation energy to be the more accurate, since the value for hydrogen was determined from a few data points measured over a narrow temperature interval. The calculated activation energies could be brought into better agreement with the measured values for tritium by modifying the Morse potential. For example, increasing the D_e parameter (stronger O-H bond) will cause $E_b(\|c)$ to increase and $E_b(\perp c)$ to decrease. However, the agreement with the measured activation energies for hydrogen as well as with the observed O-H-bond length would become poorer.

TABLE VII. Contributions from the Morse, Coulomb, and repulsive potential energy terms to the barrier height energies for the diffusion mechanisms.

	Energy (eV)		
	Morse	Coulomb[a]	Repulsion
$E_b(\|c)$	0.8004	−0.0451	0.0688
$E_b(\perp c)$	−0.245	1.158	0.317

[a] Includes the contribution in Eq. (8) from the induced dipoles on O^{2-} ions (second term) and from point charge on Ti^{4+} ions (third term).

The results of this work summarized in Tables III and IV show that reasonably good agreement with the observed equilibrium and diffusion properties of hydrogen in TiO_2 was obtained from our calculations based on the potential energy model in Eq. (8). Only the b parameter of the repulsive term of this potential was adjusted to place the O^{2-} ion at its equilibrium position in the perfect rutile lattice. The remaining parameters were fixed at values determined from other calculations or experiments on the properties of a free OH^- ion. This agreement between the calculated and observed properties is strong evidence in support of the mechanisms proposed for the diffusion of hydrogen in rutile.

ACKNOWLEDGMENT

The authors thank Dr. F. A. Modine for helpful suggestions during the early stages of this work. Research sponsored by the Division of Materials Sciences, U.S. Department of Energy under Contract No. W-7405-eng-26 with Union Carbide Corporation.

APPENDIX

The activation energy expressed in Eq. (14) takes into account the zero-point energies in the equilibrium (EC) and saddle-point configurations (SPC). The justification for Eq. (14) is based on a semiclassical statistical mechanics approach to diffusion. The diffusion coefficient from absolute rate theory is given by $D = D_0 \exp(-\Delta F/kT)$, where ΔF is the difference in free energy between EC and SPC.[29] If F and F' denote the free energy of

EC and SPC, respectively, then, within the approximation of including only modes of the proton,

$$F = V_0 - kT \ln\left(\prod_{i=1}^{3} \frac{\exp(-hc\omega_i/2kT)}{1-\exp(-hc\omega_i/kT)}\right) \quad (16a)$$

and

$$F' = V_0' - kT \ln\left(\prod_{i=1}^{2} \frac{\exp(-hc\omega_i'/2kT)}{1-\exp(-hc\omega_i'/kT)}\right), \quad (16b)$$

where V_0 and V_0' are the respective total potential energies of EC and SPC. The last terms in (16) are the vibrational partition functions (Z_v and Z_v') for the modes of the proton in EC and SPC, respectively. The exponential term of the diffusion equation is then given by

$$\exp(-\Delta F/kT) = (Z_v'/Z_v)\exp[-(V_0' - V_0)/kT]\,. \quad (17)$$

At this point, the high-temperature approximation to Z_v' and Z_v is usually taken, which gives

$$\frac{Z_v'}{Z_v} = \frac{hc}{kT}\left(\prod_{i=1}^{3}\omega_i \Big/ \prod_{i=1}^{2}\omega_i'\right).$$

However, because of the high vibrational frequencies of hydrogen in TiO_2, the high-temperature approximation is not valid. Collecting the zero-point energy contributions to the partition functions into a single term, Eq. (17) can be expressed

$$\exp\left(\frac{-\Delta F}{kT}\right) = \frac{\prod_{i=1}^{3}[1-\exp(-hc\omega_i/kT)]}{\prod_{i=1}^{2}[1-\exp(-hc\omega_i'/kT)]} \times \exp\left[\frac{hc}{2kT}\left(\sum_{i=1}^{3}\omega_i - \sum_{i=1}^{2}\omega_i'\right)\right] \times \exp\left(\frac{-\Delta V}{kT}\right). \quad (18)$$

Using the calculated values of ω_i and ω_i', it can be shown that

$$\prod_{i=1}^{3}\left[1-\exp\left(\frac{-hc\omega_i}{kT}\right)\right] \Big/ \prod_{i=1}^{2}\left[1-\exp\left(\frac{-hc\omega_i'}{kT}\right)\right] \cong 1$$

over the temperature range of the diffusion measurements. Combining the exponential terms, Eq. (18) reduces to

$$\exp(-\Delta F/kT) = \exp\{-[\Delta V - \Delta G_e(0)]/kT\}. \quad (19)$$

where,

$$\Delta G_e(0) = \frac{hc}{2}\left(\sum_{i=1}^{3}\omega_i - \sum_{i=1}^{2}\omega_i'\right).$$

It is seen that $\Delta F = \Delta V - \Delta G_e(0)$ is identical to Eq. (14), since $\Delta F = E_a$, $\Delta V = E_b$ and

$$\Delta G_e(0) = \sum_{k=1}^{3} G_{e,k}(0) - \sum_{k=1}^{2} G_{e,k}'(0).$$

---

*Present address: Metals and Ceramics Division, Owens–Corning Fiberglas Technical Center, Granville, Ohio 43023.

[1]J. B. Bates and R. A. Perkins, Phys. Rev. B 16, 3713 (1977).
[2]J. V. Cathcart, R. A. Perkins, J. B. Bates, and L. C. Manley, J. Appl. Phys. (to be published).
[3]J. B. Bates, R. A. Perkins, and J. C. Wang, Bull. Am. Phys. Soc. 23, 212 (1978).
[4]O. W. Johnson, S.-H. Paek, and J. W. DeFord, J. Appl. Phys. 46, 1026 (1975).
[5]G. R. Caskey, Mater. Sci. Eng. 14, 109 (1974).
[6]G. J. Hill, Br. J. Appl. Phys. 1, 1151 (1968).
[7]P. F. Chester and D. H. Bradhurst, Nature 199, 1056 (1963).
[8]A. von Hippel, J. Kalnajs, and W. B. Westphal, J. Phys. Chem. Solids 23, 779 (1962).
[9]J. W. DeFord and O. W. Johnson, J. Appl. Phys. 44, 3001 (1973).
[10]R. W. G. Wyckoff, *Crystal Structures*, 2nd ed. (Interscience, New York, 1964), Vol. 1, p. 251.
[11]P. I. Kingsbury, Jr., W. P. Ohlsen, and O. W. Johnson, Phys. Rev. 175, 1099 (1968).
[12]O. W. Johnson, W. D. Ohlsen, and P. I. Kingsbury, Phys. Rev. 175, 1102 (1968).
[13]B. H. Soffer, J. Chem. Phys. 35, 940 (1961).
[14]Recently (Ref. 2) we reported evidence showing that diatomic hydrogen also exists in TiO_2 at low concentrations near the surface of the crystal.
[15]P. O. Anderson, E. L. Kollberg, and A. Jelenski, Phys. Rev. B 8, 4956 (1973).
[16]As noted in Ref. 1, a shift of the OH^- stretching mode to 300 cm^{-1} or more below the free-ion value as observed in TiO_2 requires a bandwidth of 200 cm^{-1} based on correlations with linear H-bonded systems (Ref. 17).
[17]G. C. Pimental and A. L. McClellan, *The Hydrogen Bond* (Freeman, San Francisco, 1960), Chap. 3.
[18]G. Herzberg, *Molecular Spectra and Molecular Structure I. Spectra of Diatomic Molecules* (Van Nostrand, New York, 1955), Chap. 3.
[19]R. F. W. Bader in *The Chemistry of the Hydroxyl Group, Part I,* edited by S. Patai (Interscience, London, 1971), Chap. 1.
[20]P. E. Cade, J. Chem. Phys. 47, 2390 (1967).
[21]P. M. Morse, Phys. Rev. 34, 57 (1929).
[22]G. W. King, *Spectroscopy and Molecular Structure* (Holt, Rinehart, and Winston, New York, 1964), Chap 5.
[23]L. M. Branscomb, Phys. Rev. 148, 11 (1966).
[24]P. I. Kingsbury, Jr., W. D. Ohlsen, and O. W. Johnson, Phys. Rev. 175, 1091 (1968).
[25]J. R. Tessman, A. H. Kahn, and W. Shockley, Phys.

Rev. 92, 890 (1953).
[26]M. P. Tosi and F. G. Fumi, J. Phys. Chem. Solids 25, 45 (1964).
[27]The calculations were carried to six-place accuracy in the atomic positions.
[28]P. Dawson, Solid State Commun. 10, 41 (1972).
[29]C. P. Flynn, *Point Defects and Diffusion* (Clarendon, Oxford, 1972), Chap. 7.